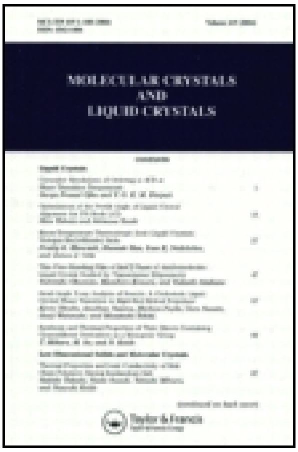

Molecular Crystals and Liquid Crystals Science and Technology. Section A. Molecular Crystals and Liquid Crystals

Publication details, including instructions for authors and subscription information:
http://www.tandfonline.com/loi/gmcl19

Shear-Induced Surface Alignment of Polymer Dispersed Liquid Crystal Microdroplets on the Boundary Layer

D. S. Parmar [a] & J. J. Singh [a]

[a] NASA Langley Research Center, Hampton, Va, 23665

Version of record first published: 24 Sep 2006.

To cite this article: D. S. Parmar & J. J. Singh (1993): Shear-Induced Surface Alignment of Polymer Dispersed Liquid Crystal Microdroplets on the Boundary Layer, Molecular Crystals and Liquid Crystals Science and Technology. Section A. Molecular Crystals and Liquid Crystals, 225:1, 183-196

To link to this article: http://dx.doi.org/10.1080/10587259308036228

Mol. Cryst. Liq. Cryst., 1993, Vol. 225, pp. 183–196
Reprints available directly from the publisher
Photocopying permitted by license only

Printed in the United States of America

Shear-Induced Surface Alignment of Polymer Dispersed Liquid Crystal Microdroplets on the Boundary Layer†

D. S. PARMAR‡ and J. J. SINGH
NASA Langley Research Center, Hampton, Va. 23665

(Received November 14, 1991; in final form April 20, 1992)

Polymer dispersed liquid crystal thin films have been deposited on a glass substrate, utilizing the processes of polymerization and solvent evaporation induced phase separation. Liquid crystal microdroplets trapped on the upper surface of the thin film respond to the shear stress due to air or gas flow on the surface layer. Response to an applied step shear stress input on the surface layer has been measured by measuring the time response of the transmitted light intensity. Initial results on the measurements of the light transmission as a function of the air flow differential pressure indicate that these systems offer features suitable for boundary layer and gas flow sensors.

INTRODUCTION

In recent years, there has been a growing interest in the study of the electro-optic effects in polymer dispersed liquid crystal (PDLC) thin (~25 μm) films[1-4] for their potential use in large area electro-optic displays and electrically controllable optical shutters. PDLC thin films consist of liquid crystal micro droplets (0.1–10 μm) dispersed randomly in polymer matrices and are formed by the processes of phase separation induced by polymerization, thermal quenching or solvent-evaporation.[5] The size distribution of the droplets is controlled, among other factors, mainly by the liquid crystal concentration and the rate of phase separation.[6,7] In its normal *off* state (in absence of external fields), the PDLC thin film scatters light strongly, resulting in a cloudy appearance. The film is sandwiched between glass plates coated with transparent conducting electrodes and becomes transparent (*on* state) on the application of a sufficiently high electric field if the dielectric anisotropy $\Delta\varepsilon$ of the liquid crystal is positive. The transparency, a function of the applied electric field, is maximum when the refractive indices of the polymer, the liquid crystal and the glass are matched. In the *off* state, scattering from a droplet depends on its size,

†Work performed under master agreement between NASA and the Old Dominion University Research Foundation, Task # NAS1-18584-111.

‡Department of Mechanical Engineering and Mechanics, Old Dominion University, Norfolk, Va. 23529-0050.

the polymer refractive index, the birefringence, and the nematic director orientation with respect to the incident light. The electric field controls the scattering cross section of the liquid crystal droplets strongly, making the PDLCs potential candidates for a variety of optical and electro-optical control and display applications.

In the conventional mode of electro-optical display operation, the PDLC thin film, comprised of droplets of a nematic liquid crystal (a birefringent object) of birefringence $\Delta \mathbf{n} = \mathbf{n}_e - \mathbf{n}_o$ ($\mathbf{n}_e$ and $\mathbf{n}_o$ being the extraordinary and the ordinary refractive indices respectively) embedded in a polymer (an isotropic medium) of carefully selected refractive index $\mathbf{n}_p$, is sandwiched between two transparent electrodes to apply external electric field. In the absence of the external electric field, the nematic droplets are inhomogeneously birefringent where the optic axis is along the local nematic director **n**. In this situation, there is a strong scattering of the incident light giving a hazy appearance to the film. On the application of a sufficiently strong electric field through the transparent electrodes, **n** aligns parallel to the field and a condition $\mathbf{n}_p = \mathbf{n}_o$ results. Consequently the PDLC thin film transparency increases. On removal of the electric field, the director **n** in each droplet tends to relax back to its own preferred direction resulting in the hazy appearance of the film again.

In the present mode of operation, however, external shear stress on a free surface of the PDLC thin film instead of electric field on a sandwich cell, has been used. Also the liquid crystal microdroplets fill randomly distributed micro voids in a rigid continuous polymer matrix providing a PDLC thin film free surface morphology in which the microdroplets on the top surface of the thin film are only partially entrapped in the polymer matrix. This results in an unique PDLC configuration where the droplets are surrounded by the rigid polymer matrix from all sides except from the top thus providing a direct liquid crystal-air interface. Such a PDLC free surface, when exposed directly to the shear stress due to air flow, responds by shear stress field induced director reorientation. These director reorientations result in an optical response when the PDLC thin film is viewed under crossed polarizers. It is in this respect that the present mode of PDLC operation is new and different from the conventional mode. In this paper, we report for the first time the observation and measurement of optical response of this new mode of operation of the PDLC thin film, deposited on a glass substrate, to an applied shear stress on the surface exposed to the wind flow. We call this mode as partially exposed polymer dispersed liquid crystals (PEPDLC) and discuss the optical transmission characteristics[8] of the PEPDLC droplets on a local as well as global level in relation to their structure.

EXPERIMENTAL

PDLC thin films are deposited on glass substrates by the method of solvent evaporation-induced phase separation. Nematic liquid crystal (E38, BDH, U.K.) is dissolved in a solution of polystyrene in 1:1 concentration of Acetone and Methyl Ethyl Ketone. The liquid crystal and polymer solution mixture has a concentration ratio of (1:1). The polymer matrix-liquid crystal mixture is sprayed on a glass

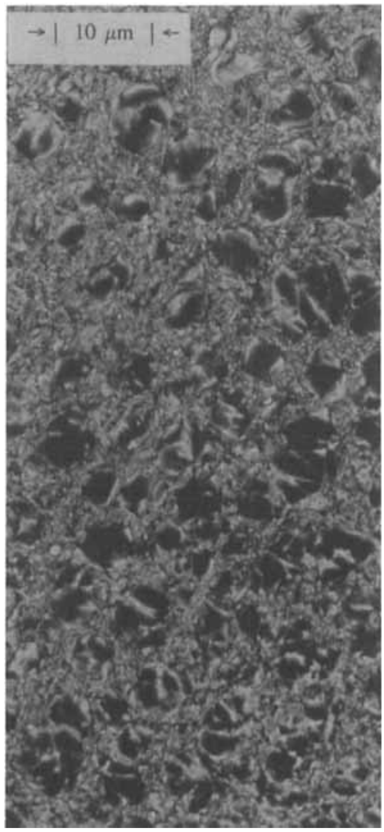

FIGURE 1 Size distribution of the nematic droplets on the exposed surface of the PDLC thin film. See Color Plate IV.

substrate to provide a dry film thickness of ~10–25 μm. As the solvent evaporates, the liquid crystal tends to become insoluble and starts phase separating from the polymer matrix in the form of the microdroplets. When the solvent has evaporated completely, a typical PDLC texture (liquid crystal droplets dispersed in a rigid polymer matrix), shown in Figure 1, is observed when viewed through crossed polarizers in a transmission microscope. In the texture of Figure 1, microdroplets with size (diameter) distribution of ~2–5 μm are partially exposed (or covered by an extremely thin and flexible polymer matrix film) on the upper surface of the PDLC thin film. Clusters of the partially exposed droplets (PED) are also seen making some of the droplets appear non spherical in shape and sizes larger than 5 μm. The top surfaces of the PEDs respond to the air flow on the PEPDLC film surface by director reorientations. The exposed surface being much smaller in comparison to the total surface area of the droplet, it is assumed that the changes in shape or in size of the PED induced by the director reorientation are insignificant and that in the present context, the exposed PED surface can be considered as flat. In the following discussions we shall refer only to the responses of the PEPDLC droplets and also assume that each droplet in a cluster behaves independently of the other. The droplets lying deeper in the bulk of the PDLC film are covered from all sides by the rigid polymer matrix and are largely unaffected by the air flow. Also, the droplets formed on the top surface of the thin film as completely free from the polymer matrix do not hold to the surface under shear stress and are washed out easily by the wind flow during first few seconds of the experiment. The results reported here do not include the response of the droplets which are washed out. Further, similarity of the optical contrast among the microdroplets under crossed polarizers in Figure 1 reveals that they have about the same distribution of director orientation.

The experimental arrangement to study the transmission of light through the PEPDLC thin film under shear stress is shown in Figure 2. For measurements of the transmitted light intensity as a function of the shear stress on a global scale, the optical arrangement of Figure 2(a) in which the light source is a white light lamp, is used. The transmission characteristics of a single isolated droplet are measured by using a He-Ne laser as shown in Figure 2(b). The PEPDLC sample is mounted on a polarizing microscope (NIKON, Optihot-Pol). Compressed air is blown horizontally over the sample and a flow measurement system consisting of a flowmeter, a differential pressure sensor, an electronic manometer and an electromagnetic valve are used to determine the flow conditions. The electromagnetic valve triggers the oscilloscope when the air is released and the variation of the transmitted light intensity as a function of time from the instant of switching on of the flow is recorded with the help of a photodetector attached to the microscope. For a known constant rate of the air flow, the sample is photographed with the microscope camera assembly.

RESULTS

Apart from the concentration of the liquid crystal in the polymer matrix, the PEPDLC droplet size is also found to be a function of the thickness of the PDLC thin film. For example, for a PDLC film thickness ~10 μm, the PED size distribution of Figure 3(a) in which size ranges from ~2–5 μm is observed. Similarly for a film thickness ~20 μm, the range of PED size is ~2–10 μm as shown in Figure 3(b). Also, in Figure 3(b), unlike in Figure 3(a), many of the PEPDLC droplets are bipolar and have varying molecular orientations, evidence of which is provided by their varying optical contrasts under crossed polarizers. Although the exact reasons for this variation in the size and the texture of the droplet with film thickness have not been identified, there are clear indications that the kinetics of the droplet formation in the vicinity of the thin film free surface are a function of its thickness. Upon establishing an air flow on the exposed surface layer, the intensity of the transmitted light through the drops increases as a function of the air flow differential pressure Δp. For the PEPDLC droplet size distribution of Figure 3(a), three such situations are shown in Figure 4(a, b, c) for Δp = 12.8, 20.1 and 36.8 Torr respectively, applied along the direction of the arrow (arranged for about 30° to the polarizer). It may be noted that the brightness of the droplet close to the tip of the arrow increases from dark at $\Delta p = 0$ [Figure 3(a)] to bright for Δp = 36.8 Torr [Figure 4(c)]. The transmission ratio, ΔI [defined as $(I_s - I)$/

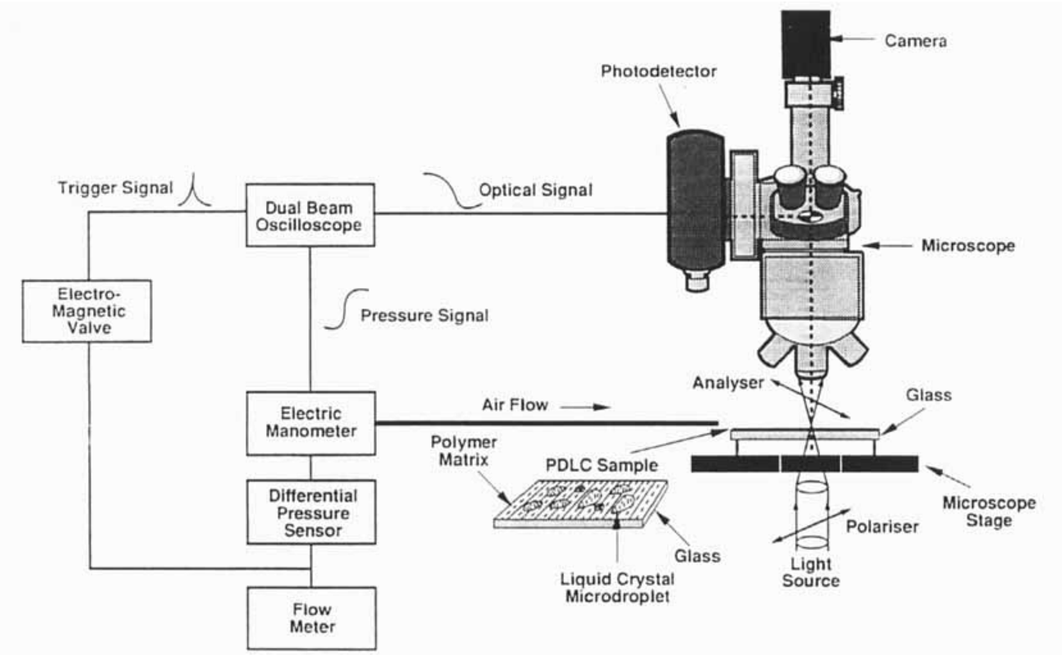

FIGURE 2(a) Schematic diagram of the experimental set up.

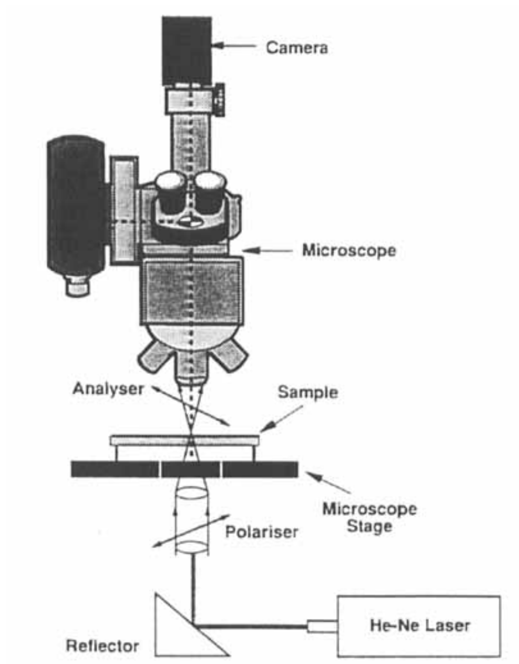

FIGURE 2(b) He-Ne laser is used for transmission through an isolated droplet.

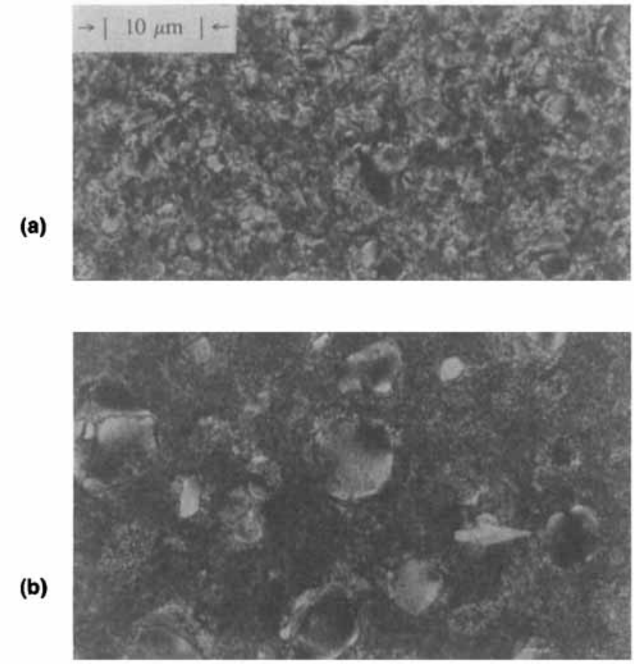

FIGURE 3 Droplet size distribution for a PDLC thin film (a) ~10 μm, (b) ~25 μm. See Color Plate V.

I, where I_s and I are the transmitted light intensities in the presence and the absence of shear stress respectively] is shown as a function of Δp in Figure 5 for three different locations in the sample. It may be noted that ΔI, after demonstrating an initial growth, shows large fluctuations beyond Δp = 40 Torr. This large dispersion in ΔI beyond Δp = 40 Torr is believed, apart from several other complex factors, to be due to the presence of a number of PEPDLC bipolar droplets. Such a behavior can be understood by considering the optical response of a bipolar droplet to an applied shear stress shown in Figure 6(a, b, c, d) for Δp = 0, 15, 40 and 60.2 Torr respectively. The corresponding director **n** distributions under the flow conditions are depicted in Figure 7 (a, b, c, d). In Figure 7, A and P are the analyzer and the polarizer (crossed) respectively. For Δp = 0 in Figure 6(a), the director **c** (the projection of **n** on the plane of the polarizers) at the center of the droplet is along A (Figure 7a) giving a dark appearance. **c** is at an angle ϕ relative to A on the left and the right (Figure 7a) of the central dark brush giving a brighter appearance in comparison to the central dark brush. When air flows over the surface in the direction of the arrow [Figure 7(b)], ϕ increases further relative to A and the dark brush moves to the right (Figure 6b) due to the Δp (= 15 Torr) induced torque on **n**. Further increase in Δp increases ϕ further relative to A (Figure 7c, Δp = 40 Torr) and a consequent shift of the dark brush further to the right (Figure 6c) is observed. For Δp beyond 40 Torr, ϕ increases relative to A but, at the same time, **c** tends to come closer to the direction of P (Figure 7d, Δp = 60.2 Torr) resulting in a fall in the brightness on the left of the droplet. For a situation in which the responses corresponding to Figures 7(c, d) for all the bipolar droplets are not in

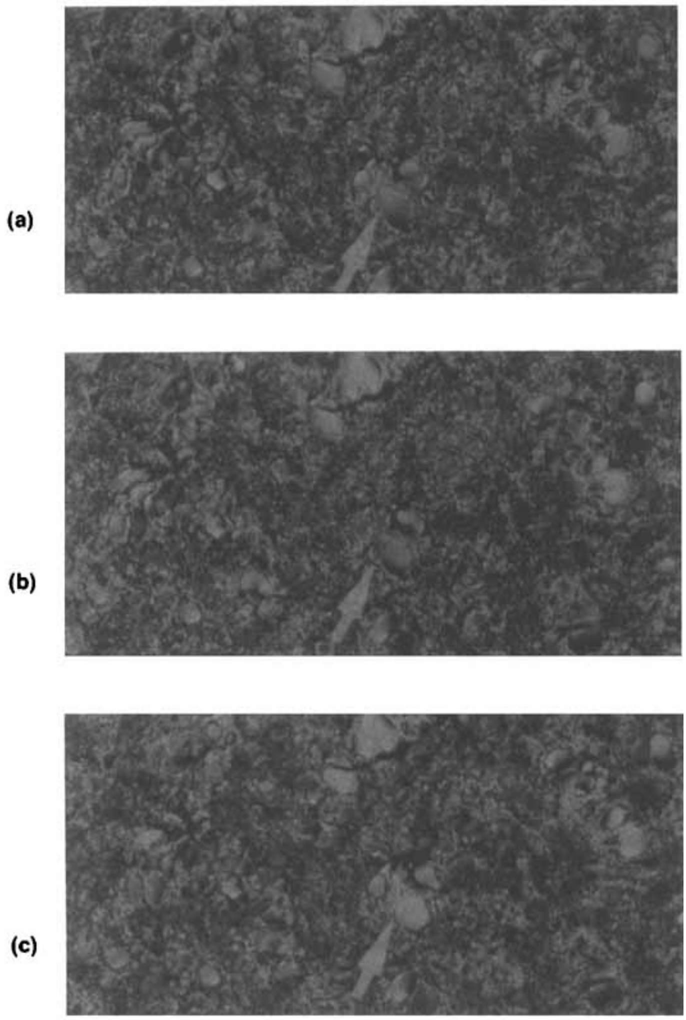

FIGURE 4 Droplets in Figure 3(a) get brighter for air flow in the direction of the arrow; Δp (Torr) (a) 12.8, (b) 20.1, (c) 36.8. See Color Plate VI.

unison, fluctuations in the transmitted light intensity are expected. Another important aspect of the director structures of Figure 7 is the appearance of defects and disclinations at the center of the PEPDLC droplet as areas of larger elastic energy for higher Δp. The dynamics of these defects, combined with the effect of the hydrodynamic flow observed at higher Δp in a number of PEPDLC droplets, contribute to the observed dispersion in Figure 5. Another most likely and important factor contributing to this dispersion in ΔI at higher Δp is the transition of the boundary layer from laminar to turbulent. Detailed investigations of this possibility of the boundary layer transition are currently underway in wind tunnel environment using PEPDLC thin films.

The optical response of the bipolar droplets is further understood from the optical

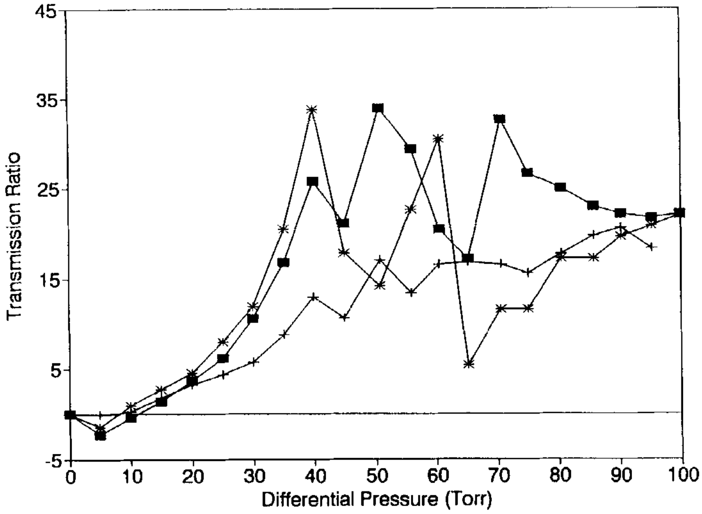

FIGURE 5 Average transmission ratio as a function of Δp for: ■, droplets of Figure 3(a), * and + for the same film but each in areas different from the field of view of Figure 3(a).

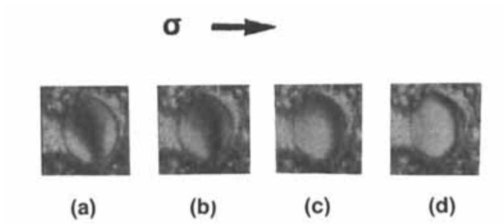

FIGURE 6 Response of a bipolar droplet of size ~8 μm to an applied shear stress (Torr) (a) 0, (b) 15, (c) 40, (d) 60.2. See Color Plate VII.

response of an isolated bipolar droplet (~8 μm) measured with the help of the optical arrangement of Figure 2(b) in which a He-Ne laser was used as the light source. The change in the brightness of the droplet as a function of the air flow Δp is demonstrated in Figure 8(a–d). In absence of the air flow ($\Delta p = 0$), the droplet is darker (Figure 8a) in comparison to that for $\Delta p = 16.5$ Torr (Figure 8b) applied in the direction of the arrow. The brightness increases further in Figure 8c for $\Delta p = 48$ Torr. Further increase in Δp generates director orientations resulting in the appearance of darker regions at the center of the droplet as shown in Figure 8d for $\Delta p = 61.7$ Torr for reasons explained above. The variation of the transmitted light intensity (transmission ratio ΔI) as a function of the differential pressure for this isolated bipolar droplet is shown in Figure 9. ΔI shows an initial exponential type of growth with Δp and starts falling beyond $\Delta p = 40$ Torr. ΔI increases again beyond $\Delta p = 85$ Torr when the black areas at the center of the droplet in Figure 8d move to the boundaries due to increased shear stress. Although some light passes also through the polymer matrix surrounding the droplet in Figure 7, these contributions are subtracted out in the normalization scheme for ΔI and consequently Figure 9 represents the response from the PEPDLC droplet only.

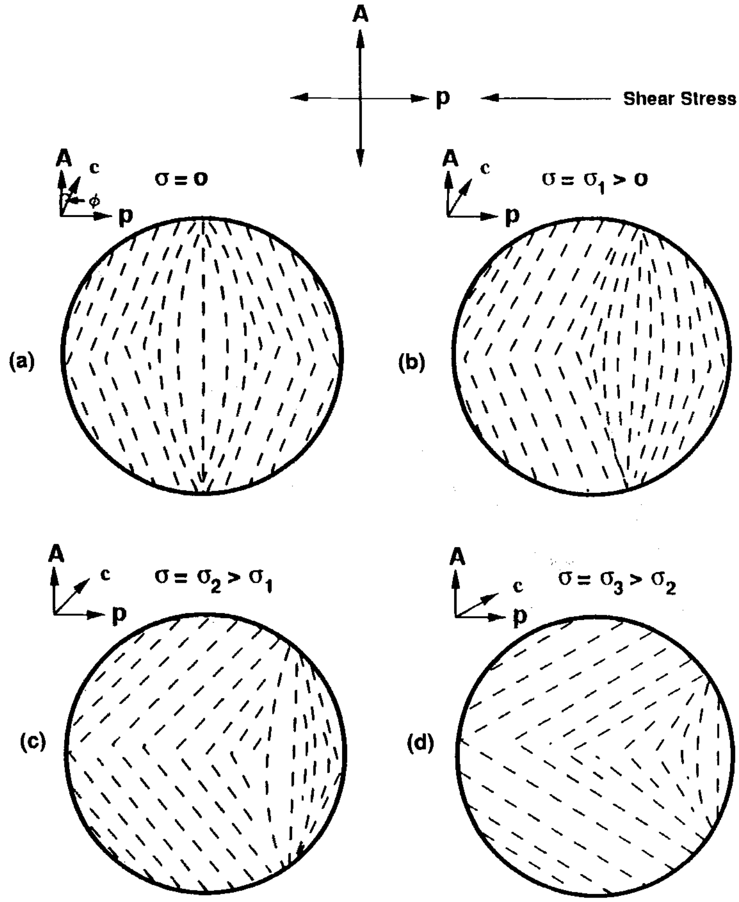

FIGURE 7 Representative director orientations in the bipolar droplet in four different situations of Figure 6. Director orientations of the dark and the bright areas have been shown.

DYNAMICS OF THE DIRECTOR IN THE DROPLET

The equation of motion of the director under the applied shear stress can be solved from free energy considerations. In the coordinate system of Figure 10 where the director **n** makes an angle θ with the z-axis and the polarizer and the analyzer are aligned along the y- and the x-axes, respectively, the total free energy F of the droplet in the presence of Δp may be written as the sum of contributions from the elastic deformation, F_{elast}, the shear stress, F_{shear} and the anchoring on the surfaces, F_{anch}; i.e.

$$F = F_{\text{elast}} + F_{\text{shear}} + F_{\text{anch}} \tag{1}$$

The three contributions to the total free energy density of the nematic droplet may be calculated, from first principles,[9] as:

$$F_{\text{elast}} = \tfrac{1}{2} k_{11}(\nabla \cdot \mathbf{n})^2 + \tfrac{1}{2} k_{22}(\mathbf{n} \cdot \nabla x \mathbf{n})^2 + \tfrac{1}{2} k_{33}(\mathbf{n} x \nabla x \mathbf{n})^2 \tag{2}$$

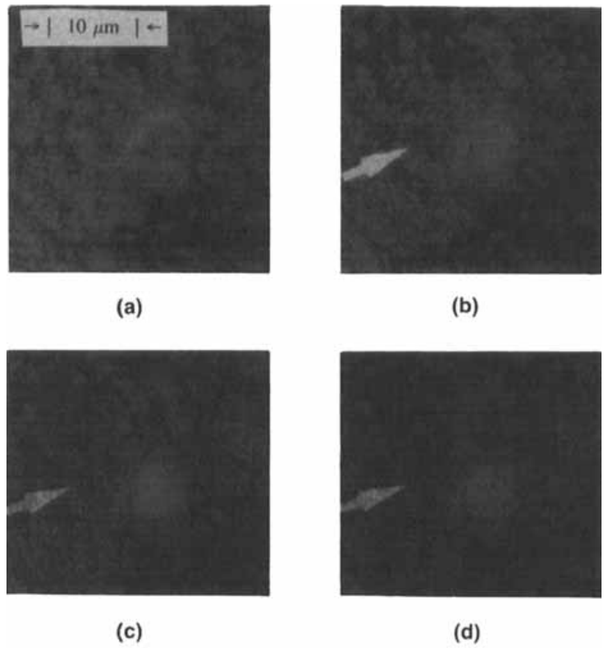

FIGURE 8 Transmission ratio as a function of Δp for an isolated bipolar droplet using He-Ne laser. Δp (Torr) (a) 0, (b) 16.5, (c) 48.0, (d) 61.7. See Color Plate VIII.

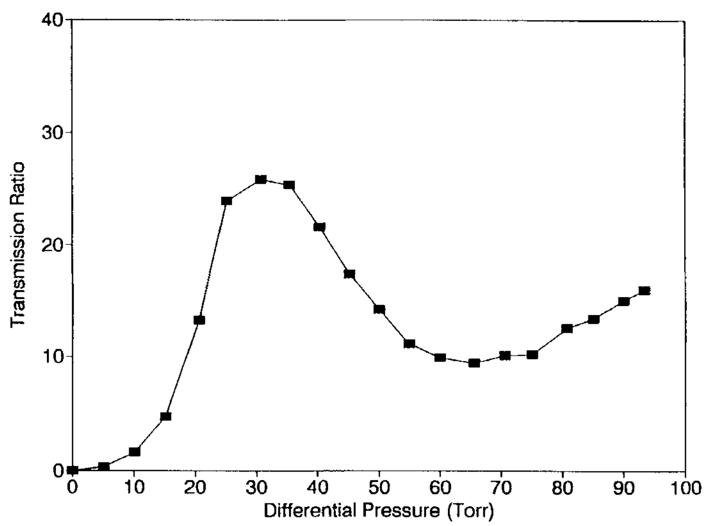

FIGURE 9 Transmission ratio as a function of Δp for an isolated bipolar droplet in Figure 8.

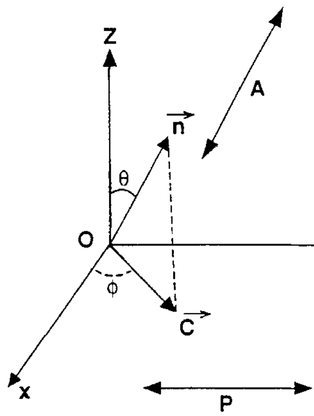

FIGURE 10 Coordinate system for the director orientation relative to the Δp. P and A are the two polarizers, $\mathbf{n}$, the director and $\mathbf{c}$, is the projection of $\mathbf{n}$ in the x-y plane.

where the first, second and third terms in Equation (2) represent respectively the conventional contributions from the splay, twist and the bend deformations. The shear stress due to Δp tends to orient $\mathbf{n}$ along itself and the free energy due to shear stress, calculated from the drag introduced on the surface area of the droplet after normalization can be written as:

$$F_{\text{shear}} = \tfrac{1}{2}\,\Delta p(\sigma \cdot \mathbf{n})^2 \tag{3}$$

where σ is the unit vector along the shear stress and for a given σ, $(\sigma \cdot \mathbf{n})^2$ shows the equality $\mathbf{n} = -\mathbf{n}$. The energy density due to anchoring on the droplet surface of area $\mathbf{A}$ may be written as:

$$F_{\text{anch}} = \tfrac{1}{2}\,\mathbf{A}\boldsymbol{\Omega}_0 \sin^2(\theta - \theta_0) \tag{4}$$

where Ω_0 is the Rapini-Papoular constant for the energy of anchoring[10] and θ_0 is the apparent angle at the surface. The total free energy F is obtained by substitution of contributions from Equations (2–4) in Equation (1):

$$F = \frac{1}{2}\int [k_{11}(\nabla\cdot\mathbf{n})^2 + k_{22}(\mathbf{n}\cdot\nabla x\mathbf{n})^2 + k_{33}(\mathbf{n}x\nabla x\mathbf{n})^2]\,dV + \frac{1}{2}\int \Delta p(\sigma\cdot\mathbf{n})^2\,dV + \frac{1}{2}\,\boldsymbol{\Omega}_0 \sin^2(\theta - \theta_0)\,d\mathbf{A} \tag{5}$$

Equation (5) can be solved in the commonly used one elastic constant approximation $k_{ii} = K$ (the boundary effect being included in the energy of anchoring), and assuming that in the range of Δp of the present experiment, the change in tilt θ due to shear stress is negligible in comparison to that in the orientation ϕ. We further assume that the exposed surface of the PEPDLC droplet, being small, is flat and remains undeformed by the applied shear stress and that the anchoring at the polymer matrix-liquid crystal interface is strong to let the director respond to the torque due the shear stress. With these assumptions, the Euler-Langrange equation and the balance between the torques due to elasticity, viscosity and the shear stress[11] (neglecting the small inertial torque), the time variation of the rotation of the director due to applied differential pressure Δp is written as:

$$\log\{\tan(\phi/2)/\tan(\phi_0/2)\} = (\Delta p'/\eta)t \quad (6)$$

where $\Delta p' = \Delta p \mid n \mid \sin^2\theta$, η is the relevant coefficient of orientational viscosity of the nematic and ϕ increases from ϕ_0 at $t = 0$ to saturate after a characteristic time t.

The dynamic response of the average intensity of the transmitted light through the PEPDLC thin film for an applied step input Δp is shown in the oscillograms of Figure 11. In Figure 11(a), the shear stress ($\Delta p = 26$ Torr) represented by the upper trace is removed at time A. The transmitted light intensity (lower trace) starts falling at the same time and the fall is complete in about 100 ms. The shear stress step input ($\Delta p = 26$ Torr) is applied again at point B resulting in the simultaneous increase in the transmitted light intensity ΔI which saturates again in about 100 ms. In Figure 11(b), on the other hand, application of an step shear stress input $\Delta p = 42$ Torr at point A (upper trace) increases the transmitted light intensity ΔI to maximum in about 40 ms. ΔI, instead of saturating after a time t

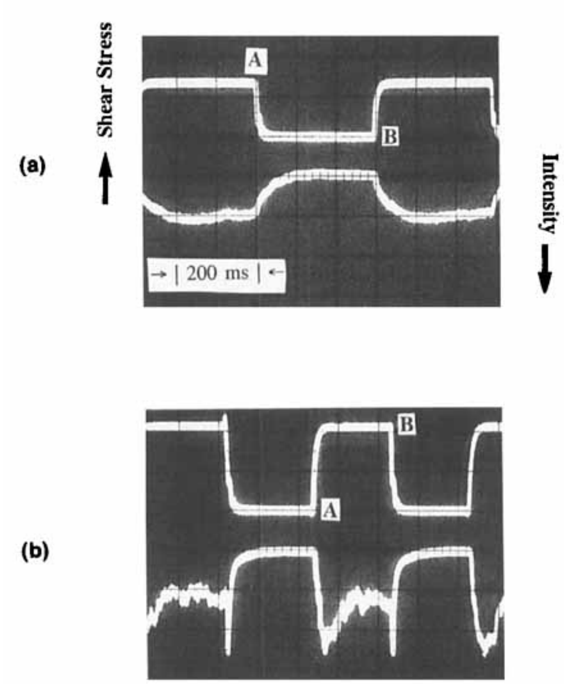

FIGURE 11 Dynamic response of the PDLC film to an applied shear stress (Δp in Torr) (a) 26, (b) 42. The arrows represent the direction of increase in shear stress (upper trace) and the transmitted light intensity (lower trace).

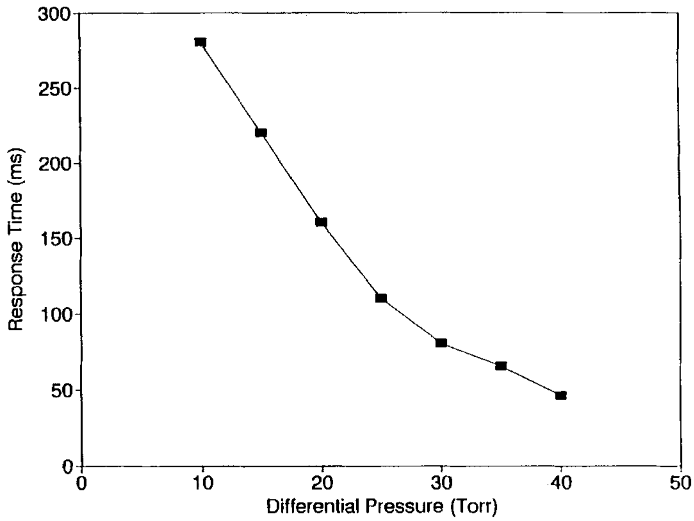

FIGURE 12 Variation of the dynamic response time τ as a function of Δp.

as in Figure 11(a), fluctuates during the entire time Δp is on until point *B*. These fluctuations in the saturated ΔI are seen clearly in the behavior of the Δp vs. ΔI curve of Figure 5 beyond $\Delta p = 40$ Torr. Withdrawing Δp at point *B* to zero in Figure 11(b) brings ΔI to zero and no fluctuations in the ΔI are observed during this time. This behavior repeats each time Δp is applied and removed subsequently in steps. The response time τ of the PDLC film, defined as the time taken from the instant of the application of Δp to the time for saturation of ΔI decreases for increasing Δp. Typical variation of τ with Δp is shown in Figure 12.

Based on the Rayleigh-Gans approximation for the light scattering from a system of birefringent particles, Žumer and Doane[12] have determined that the differential cross sections of the birefringent droplets depend strongly on the angles of incidence and scattering. The average effective total scattering cross section $\langle\rho\rangle$ from these calculations is:

$$\langle\rho\rangle = \rho_0(1 - k\zeta) \tag{7}$$

where ρ_0 is the cross section in absence of the external perturbation, κ is the parameter related to the refractive indices of the material and ζ is the measure of the degree of alignment caused by the external force. In the present case where the indices are not matched, the transmittance ΔI of the PDLC film of thickness *d* from these calculations can thus be expressed as:

$$\Delta I = e^{-\alpha\langle\rho\rangle d} \tag{8}$$

where α is a constant. Although determination of the scattering parameters is beyond the scope of the present investigations, Equation (8) in conjunction with Equation (7) explains the initial variation of ΔI with Δp in Figures 5 and 9. The

PEPDLC thin films used in the present mode thus have the potential of being used for the quantitative measurements of the boundary layer parameters in wind tunnel applications.

Acknowledgment

The authors with to thank E. M. Industries for supply of E38 used in the present experiments.

References

1. J. W. Doane, N. A. Vaz, B.-G. Wu and S. Žumer, *Appl. Phys. Lett.*, **48**, 269 (1986).
2. P. S. Drzaic, *J. Appl. Phys.*, **60**, 2142 (1986).
3. G. P. Montgomery, Jr. and N. A. Vaz, *Appl. Opt.*, **26**, 738 (1987).
4. J. W. McCargar, J. W. Doane, J. L. West and T. W. Anderson, *Proc. SPIE*, **1455**, 54 (1991).
5. J. L. West, *Mol. Cryst. Liq. Cryst.*, **157**, 427 (1988).
6. G. W. Smith and N. A. Vaz, *Liq. Cryst.*, **3**, 543 (1988).
7. G. P. Montgomery, Jr., J. L. West and W. Tamura-Lis, *Proc. SPIE*, **1455**, 45 (1991).
8. R. Ondris-Crawford, E. P. Boyko, B. G. Wagner, J. H. Erdmann, S. Žumer and J. W. Doane, *J. Appl. Phys.*, **69**, 6380 (1991).
9. P. G. deGennes, *The Physics of Liquid Crystals* (Clarendon, Oxford, 1974).
10. J. H. Erdmann, S. Žumer and J. W. Doane, *Phys. Rev. Lett.*, **64**, 1907 (1990).
11. D. S. Parmar, *Rev. Sci. Instrum.*, **62**, 474 (1991).
12. S. Žumer and J. W. Doane, *Phys. Rev. A*, **34**, 3373 (1986).